Journal of Applied Engineering, Technology and Management (JAETM)

Broken Rotor Bar Fault Detection in Induction Motors Using Motor Current Signature Analysis (MCSA)

Chenga Dorji[1*] and Jamyang Choeda[2]

[1-2]*Department of Electrical and Electronics Engineering, Jigme Namgyel Engineering College, Dewathang*

[*]*Corresponding author: Chenga Dorji, chengadorji.jnec@rub.edu.bt*

Published: June 2025

DOI: https://10.54417/jaetm.v5i1.147

Abstract

Induction motors are commonly used in various industrial applications due to their reliability and robustness. However, they are susceptible to faults that can compromise their performance and efficiency. One of the common faults encountered in induction motors is Broken Rotor Bars, which can lead to rotor imbalance, increase vibration, and reduce the efficiency of the motor. Detecting and diagnosing this fault is critical to ensure the proper operation of the motors for industrial purposes and prevent costly downtime. This paper investigates the comparative current signature analysis of Broken Rotor Bar (BRB) fault detection in induction motors using different windowing functions. The study explores the effectiveness of various windowing functions including Hanning, Hamming, Blackman, and Flattop, in enhancing the analysis of stator current signals for fault detection purposes. The analysis is conducted using Fast Fourier Transform (FFT) techniques. The findings provide insights into the impact of windowing functions on fault detection performance and suitability for motor maintenance applications, specifically in detecting faults such as broken rotor bar faults in induction motors.

Keywords— Induction motors, Broken Rotor Bar (BRB), Fast Fourier Transform (FFT), Windowing functions

1 Introduction

All machines, no matter how well they are designed, calculated, tested, and produced, inevitably face the prospect of failure at some point in their existence. Induction motors are widely used in majority of the industrial applications and in almost every field dealing with electrical power. Most motors are characterized by simplicity, efficiency, and exceptional robustness ensuring a very high degree of reliability.

However, if the condition of the machine in use is not properly monitored, maintained and the operational condition of the machines is left unchecked, exposing them to potential failures may

pose a large economic and safety risk, even the minor faults which are not important can end in catastrophic measures. This underscores the necessity for proactive maintenance strategies to mitigate the adverse consequences associated with machine failure.

Although, the induction motor is rugged, cheap, requires less maintenance, smaller in size, efficient, and operates with an easily available power supply. The study of the construction and working of the induction motor shows that the most vulnerable parts for the fault in the induction motor are the bearing, stator winding, rotor bar, and shaft. In addition, the faults are also caused by the non-uniformity of the air gap between the stator and the rotor of the induction motor. Generally, the faults in induction motor can be categorized as electrical-related faults, mechanical-related faults and environmental-related faults.

2 Broken Rotor Bar Faults

Induction motors, despite being one of the most reliable electrical machines, they are susceptible to many electrical and mechanical faults. Some research papers shows that the percentage of rotor faults is around 5-10 percent including broken rotor bar faults [1]. Another research paper found that the share of the stator faults in induction machine failure is around 50 percent, for the rotor it is 20 percent as well, and for mechanical failures and other faults accounts for 10 percent [6]. This article mainly focuses on broken rotor Bar detection in Squirrel cage induction motors as this type of fault is common in Squirrel Cage induction motors (SCIM). Regardless of the winding connection, rotors are made of skewed laminated solid metal which are arranged around its cylindrical surfaces. The laminated bar and endings can sometimes crack or break, resulting in the fault called Broken Rotor Bar (BRB) Faults.

Broken rotor bar faults are mainly caused due to overloading of motors, stresses such as dynamic stresses due to voltage fluctuations, variations in mechanical loading and shaft torque oscillations, magnetic stresses due to unbalanced magnetics pulls, mechanical stresses due to wear and tear in the motor parts and bearing failures, residual stresses due to poor quality rotor manufacturing and environmental stresses due contamination of rotor bodies by chemical and moisture. BRBs faults can be a serious problem if the induction motor is to be employed to perform the hard-duty cycles. Some of severe secondary effects of BRB faults are sparkling which is serious concern in hazardous areas, rotor core damages due to additional current passing in the healthy rotor bars and causes wear and tear bearings and other driving components.

The BRBs can also lead to shaft vibration, and thus bearing failures airgap eccentricity, and so on. Therefore, early detection is essential not only for rotor protection but also to prevent other types of motor failures. These effects shorten the life of the induction motor thus, early detection of Broken Rotor Bar is essential. The most prominent effect of a broken bar is the appearance of sideband components [3]. These sidebands are found in the power spectrum of the stator current on the left and right sides of the fundamental frequency component.

The electrical and magnetic asymmetries in the rotor cage of induction motor causes the lower sideband components, while the consequent speed ripples due to torque pulsations causes the right sideband.[5]. The frequency of these sidebands is given by:

$$flsb = (1\text{-}2ks)Hz \tag{1}$$

$$frsb = (1\text{-}2ks)Hz \tag{2}$$

Where f is the supply frequency, $K=1$ for principal harmonic, $flsb$ and $frsb$ are left and right sideband components, s= per unit motor slip. Studying the harmonics content of waveforms using the Fast Fourier Transform (FFT) is effective because FFT is a fast and affordable tool that operates in both the time and space domain. The common equation for the Fourier transform is given as [6]:

$$(F(\omega) = F[f(t)] = \int_{-\infty}^{+\infty} f(t)e^{-j\omega t}, dt \tag{3}$$

Where F is the Fourier transform operator, ω is the rotational frequency and $j = \sqrt{-1}$ is the imaginary unit.

One can assess the average dB difference between the fundamental frequency of current and the two sidebands to measure the condition of the rotor cage and identify the number of Broken Bars. The number of broken bars can be calculated by using equation (4) [6]:

$$N \approx \frac{2R}{\frac{d}{10^{20}} + \frac{p}{2}} \tag{4}$$

Where N, is the estimated number of broken bars, R is the number of slots in the rotor, d is the average dB difference between the f and the $\pm 2Sf$ sidebands, and p is the number of the poles of the motor.

3 FAST FOURIER TRANSFORM (FFT)

The Fast Fourier Transform (FFT) is a computational algorithm used to efficiently compute the Discrete Fourier Transform (DFT) of a sequence of data points. DFT converts a time-domain signal into its frequency-domain representation revealing the spectral components present in the signal [4].

After reviewing the research paper in the context of detecting Broken Rotor Bar faults in induction motors, FFT is often used to analyze the stator current signals. If the rotor bar is broken, it will introduce asymmetry in the rotor cage which will change the magnetic field distribution and later it may affect the stator current [2]. This asymmetry generates harmonics of the fundamental frequency which represents a sideband around the supply frequency in the frequency spectrum of the stator current.

Analysis of the articles reveals that the appearance of sidebands along with their relative amplitudes and frequencies will provide valuable information about the characteristics of the faults. Therefore, this technique is used to observe the sidebands to detect and diagnose various motor faults including Broken Rotor Bars (BRBs).

Illustration of the sidebands of the amplitude difference depicted in the current spectra shown by the broken rotor bar is provided in the following figures (1), (2) and (3).

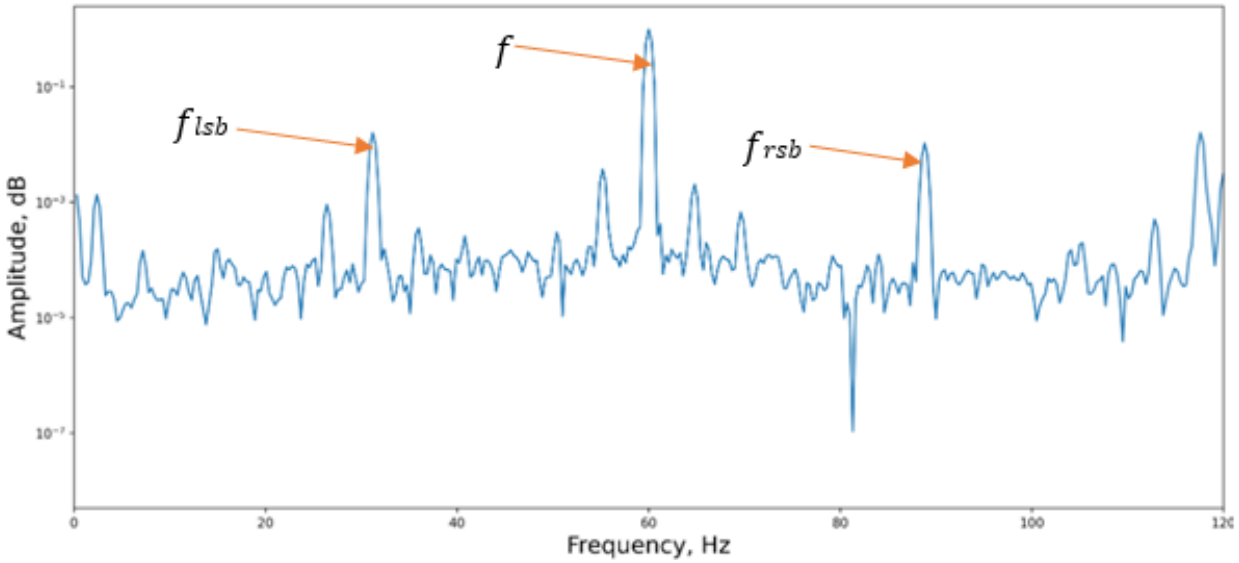


Figure 1: Current frequency components around the fundamental harmonic of $50Hz$ for Healthy State under full load

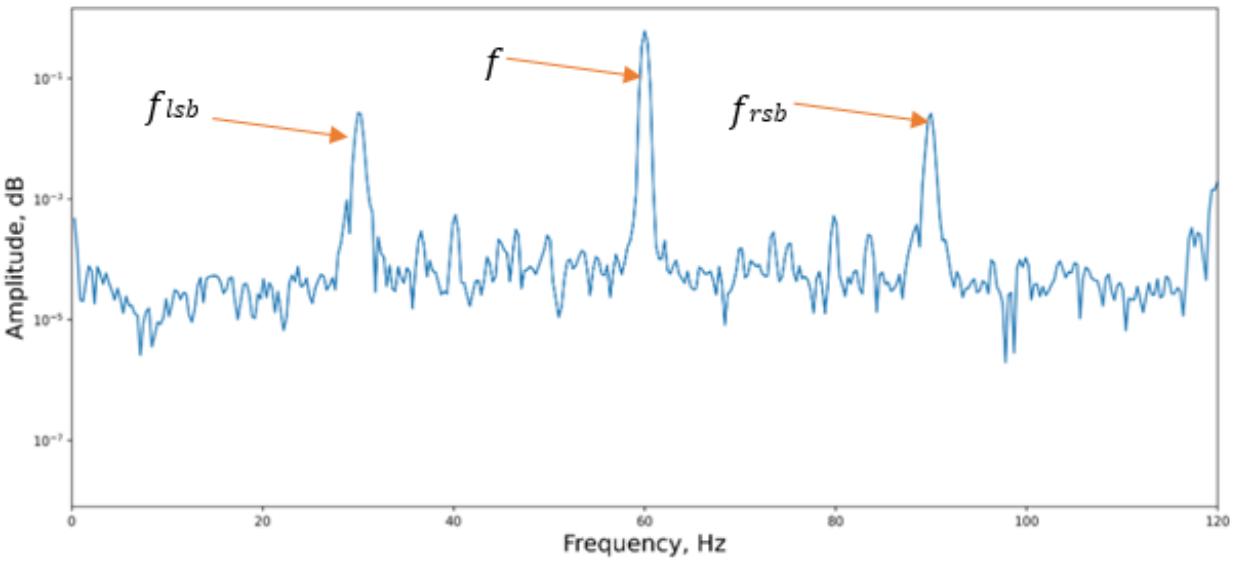


Figure 2: Current frequency components around the fundamental harmonic at minimum load for 3BRBs

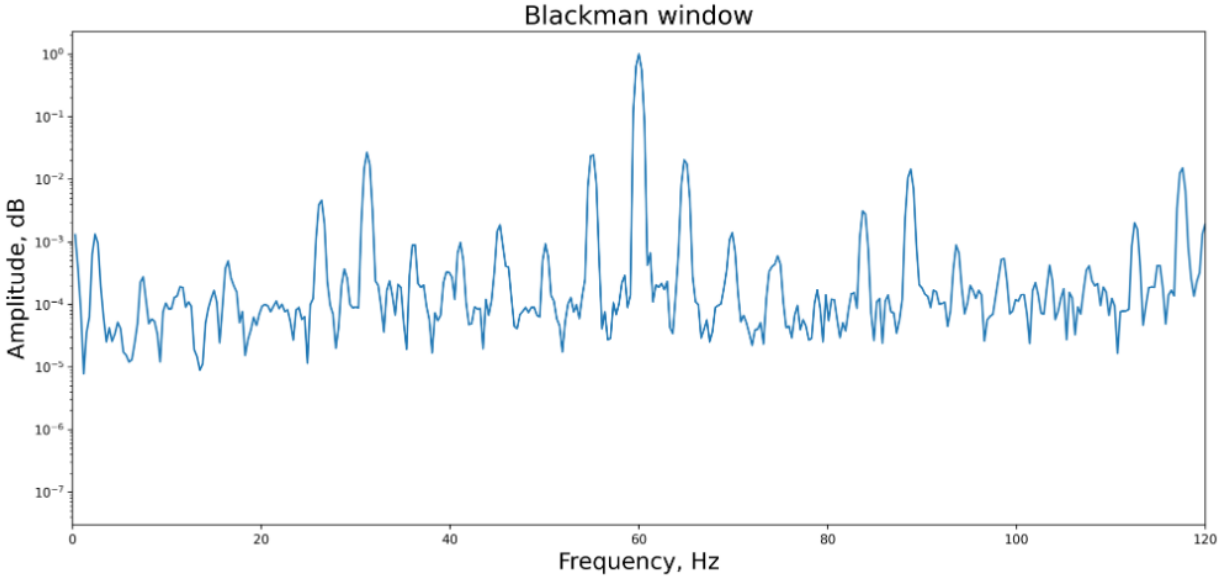


Figure 3: Current frequency components around the fundamental harmonic of 50Hz for 3 BRBs under full load level.

The above Figures simply show the comparison between the sidebands formed in the frequency spectrum during the presence of the Broken Rotor Bar faults under minimum load level and full load level. Therefore, this article compares the current frequency signals formed during the healthy state and the presence of BRB under different load levels using various windowing functions such as Hanning, Hamming, Blackman, and Flattop windows.

4 Methodology

Experiments and practical were conducted in the SCIM in the laboratory at various percent of loading to study the BRB faults in induction motor. This paper investigates the comparative

current signature analysis (CSA) of Broken Rotor Bar (BRB) fault detection in the induction motor using different Fast Fourier Transforms (FFT) windowing functions. Some of the software and tools used in analysing the BRB faults are Visual Studio Code (VS code) and Python program were downloaded and installed.

The main objectives of this paper are to: evaluate the efficacy of different windowing functions, compare frequency spectra generated by different windowing functions, determine the optimal windowing function for BRB fault detection and observe how the load level affects the generated spectra.

4.1 Experiments

4.1.1 Current Signals

The current signature analysis when the motor is in a healthy state and when the motor has a Broken Rotor Bar (BRB) under minimum load and 100 percent load level are shown in Figure 4, 5, and 6.

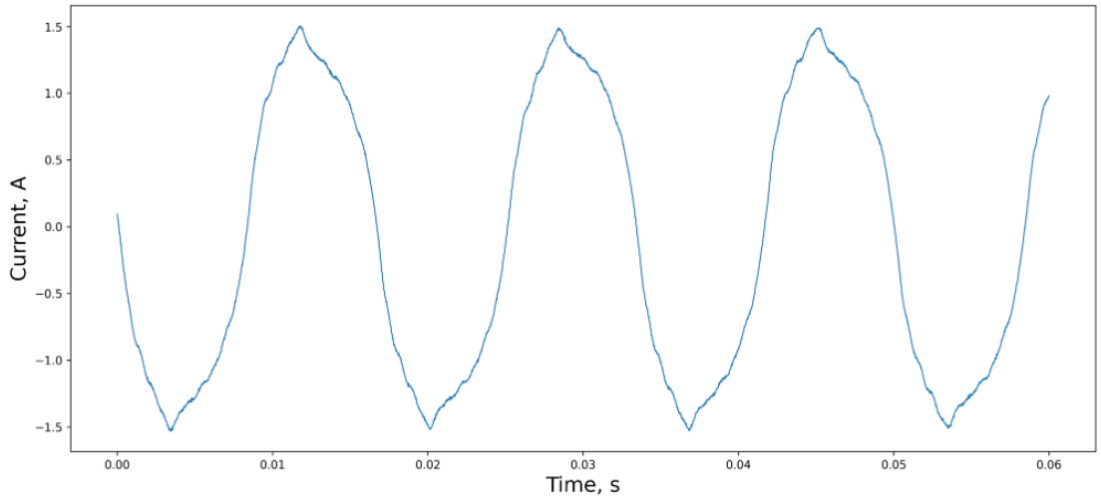


Figure 4: Current signal at a healthy state with minimum load level

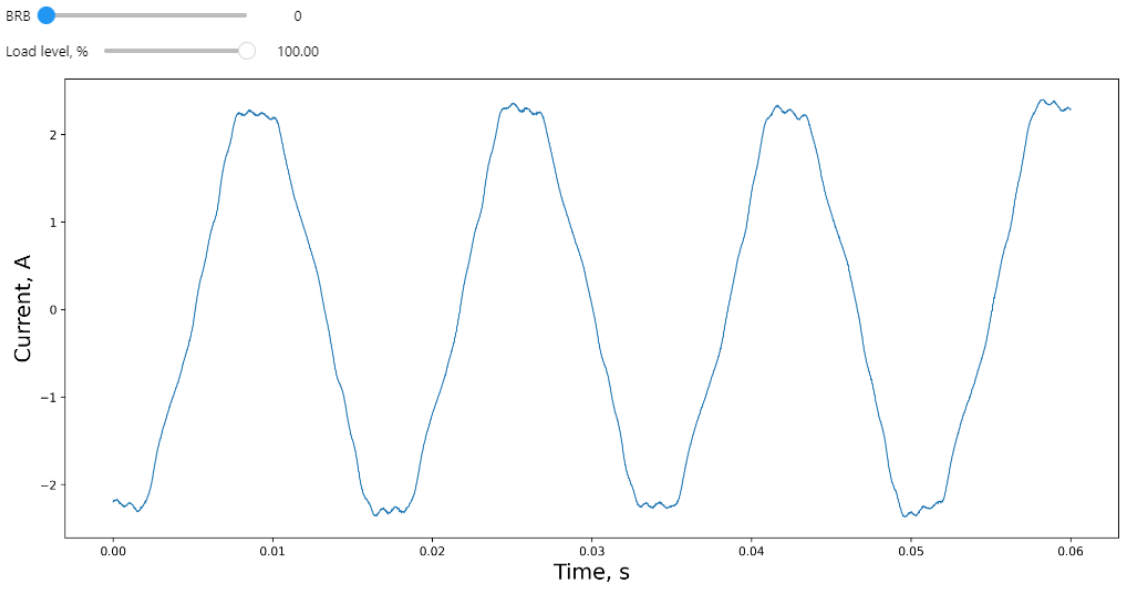


Figure 5: Current signal at a healthy state with 100% load level

When the load is full under a healthy motor in Figure 5, more pronounced harmonics are typically generated in the current signals compared to the signals observed in Figure 4 with a minimum load level. This can be due to the high current drawn by the motor which can lead to greater stresses on the motor and increase non-linear behavior which result in significant distortions in the current waveform.

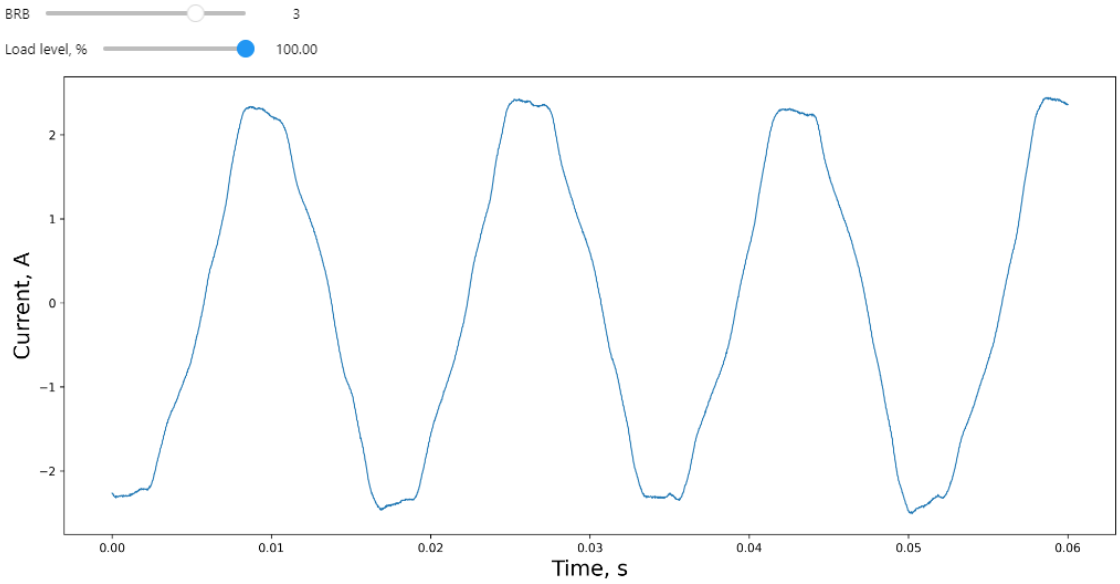


Figure 6: Current signal having 3 BRBs with 100% load level

Additionally, when the three broken rotor bars (BRBs) are introduced in Figure 6, the harmonic frequencies become more challenging to identify or distinguish. This may be because the broken rotor bar introduces additional spectral components making it difficult to isolate the individual harmonics in the FFT current signal.

4.1.2 Applying Window Functions

After reviewing numerous research papers, to use the FFT for fault detection, the stator current signal is first sampled over some time. This sampled signal is then windowed to reduce spectral leakage and improve frequency resolution. Windowing functions such as Hanning, Hamming, Blackman, and Flattop are used for this purpose. These windowing functions can taper the signal at the edges to reduce the discontinuities that can introduce unwanted frequency components during FFT analysis.

Spectral leakage refers to the spread of energy from one frequency bin to neighboring bins in the frequency domain, typically caused by windowing functions used in processing [5]. It is considered negligible because its effects are minimal and do not significantly distort the frequency analysis.

The comparison of the current frequency spectrum is made between healthy state and 3 BRBs of induction motor by applying different windowing functions as shown in figure 5 and 6 respectively.

Figure 7, 8, 9, 10, and 11 shows the current frequency spectrum of FFT when the motor is under a healthy state at full load (100% load):

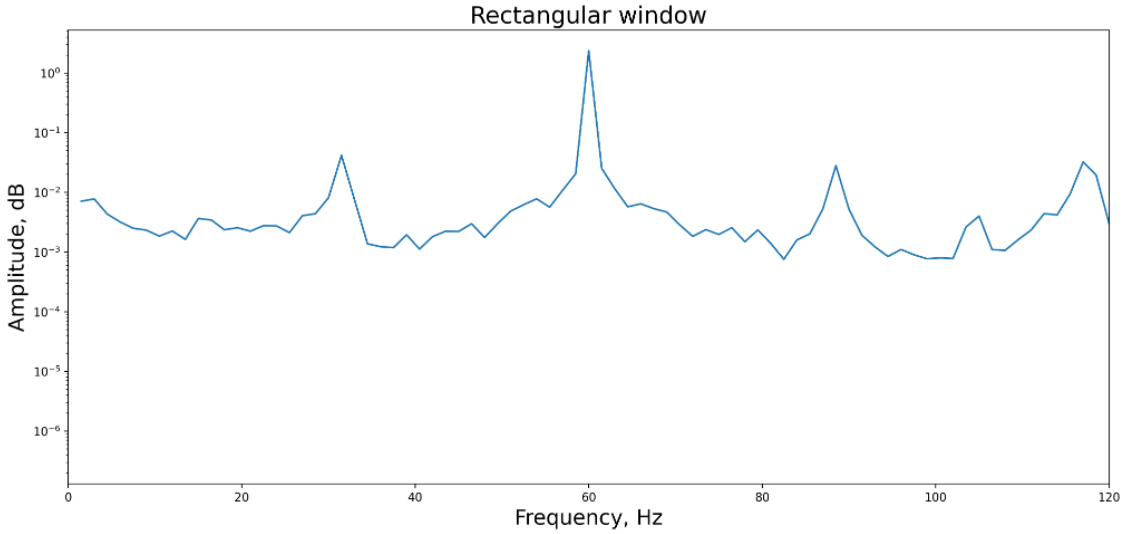


Figure 7: Rectangular window current frequency spectrum of the motor under a healthy state at full load

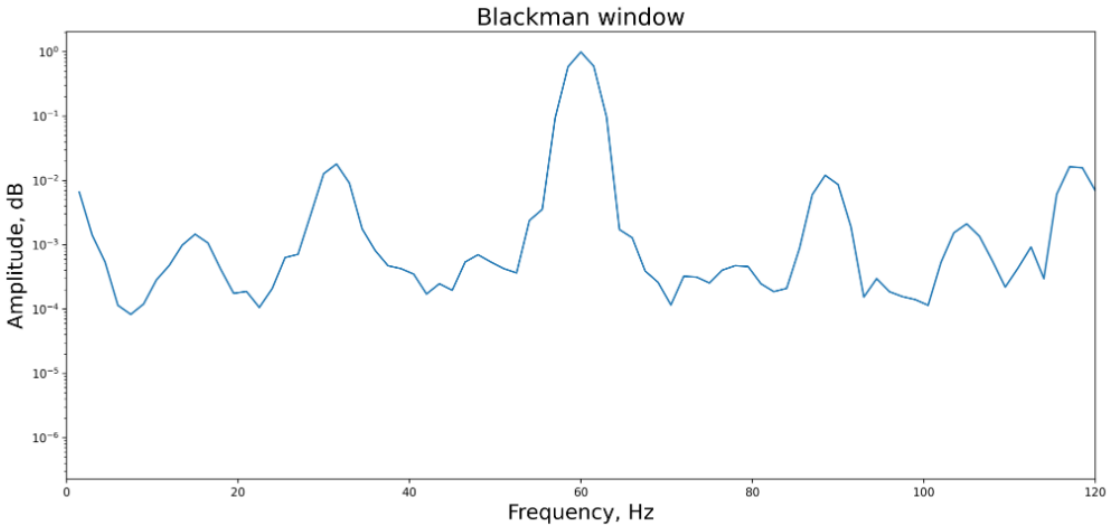


Figure 8: Blackman window current frequency spectrum of the motor under a healthy state at full load

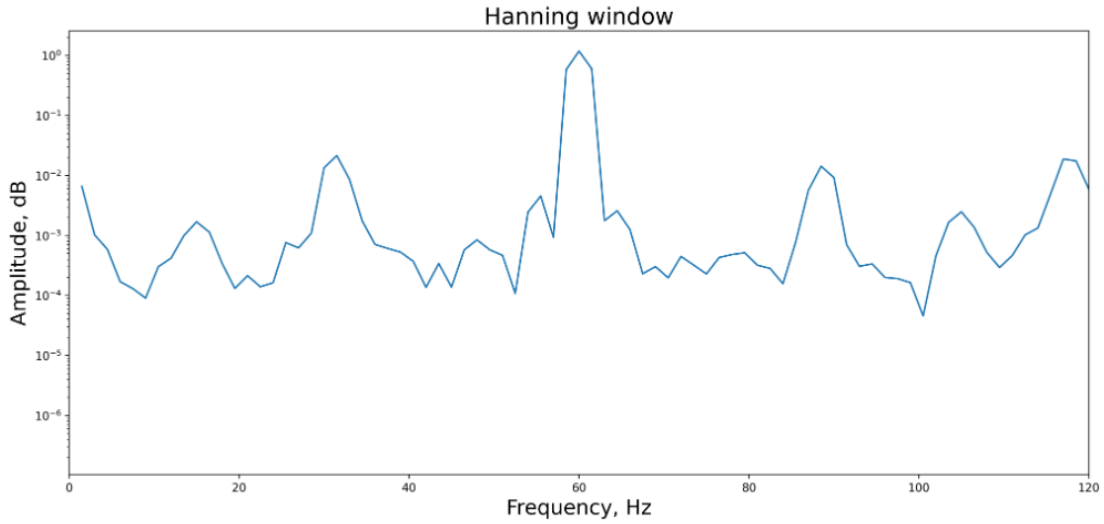


Figure 9: Hanning window current frequency spectrum of the motor under a healthy state at full load

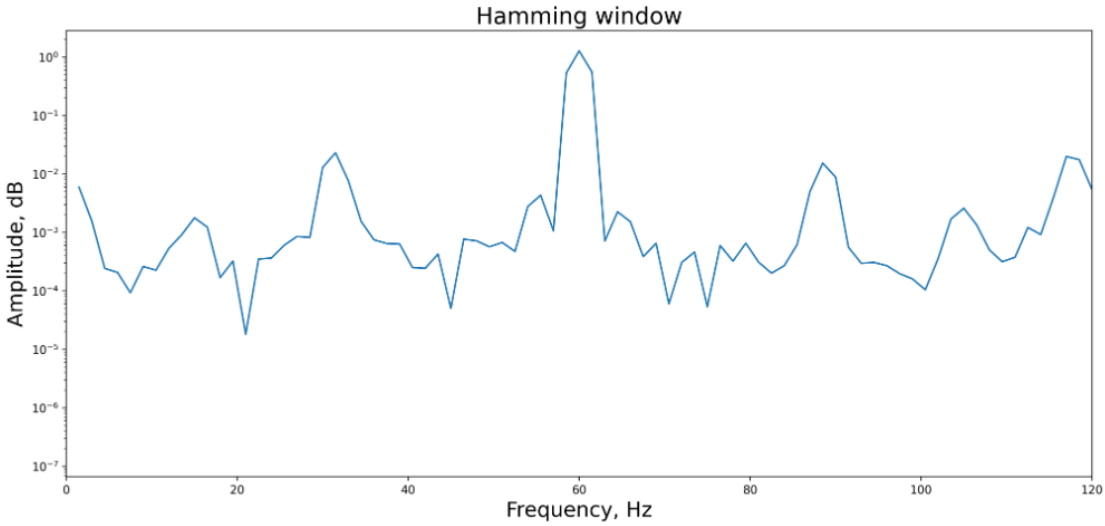


Figure 10: Hamming window current frequency spectrum of the motor under healthy state at full load

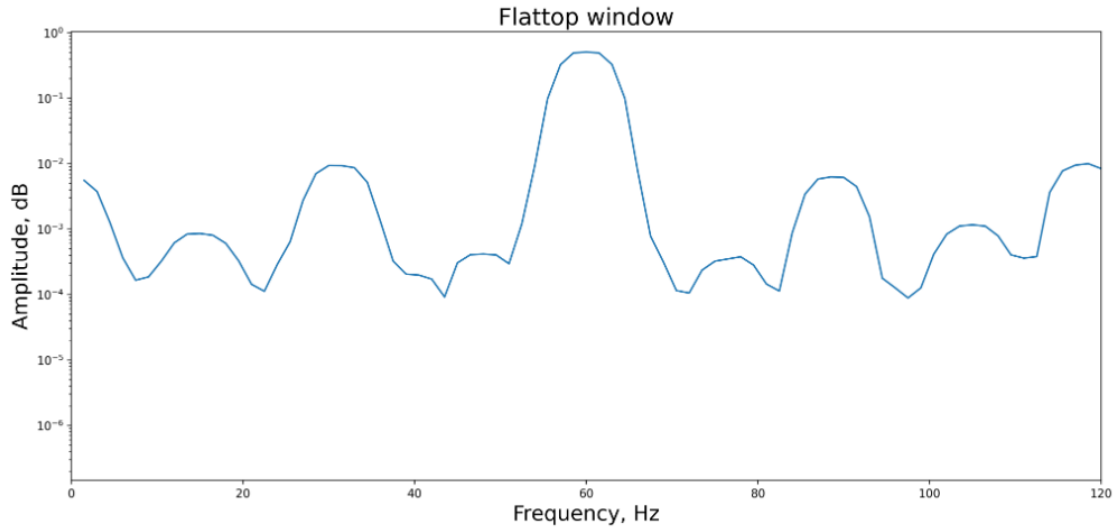


Figure 11: Flattop window current frequency spectrum of the motor under a healthy state at full load

Figure 12, 13, 14, 15, and 16 shows the current frequency spectrum of FFT at full load under 3 BRBs applying different windowing functions.

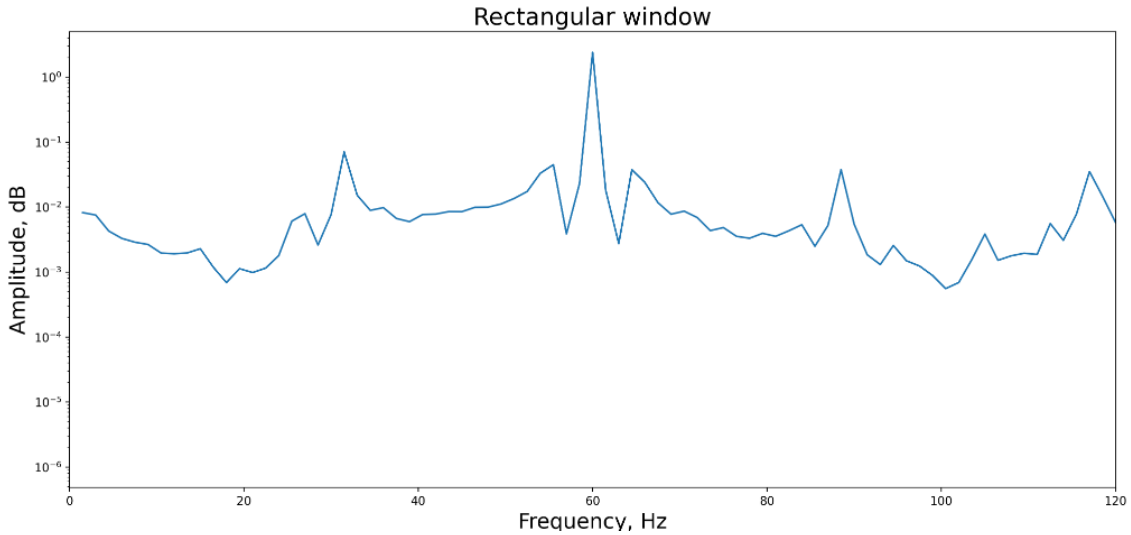


Figure 12: Rectangular window current frequency spectrum at 3 BRB

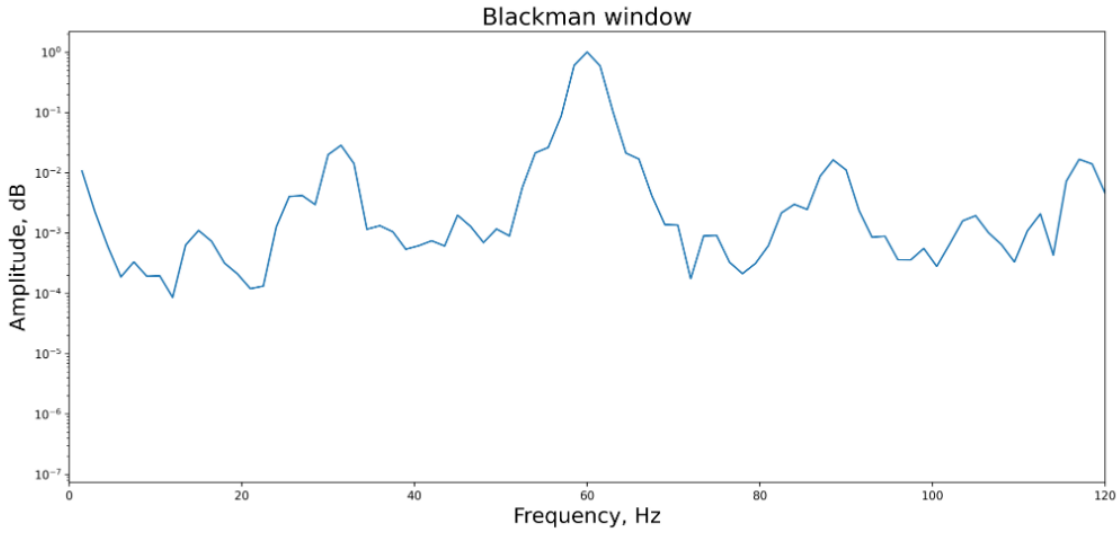


Figure 13: Blackman window current frequency spectrum at 3 BRB

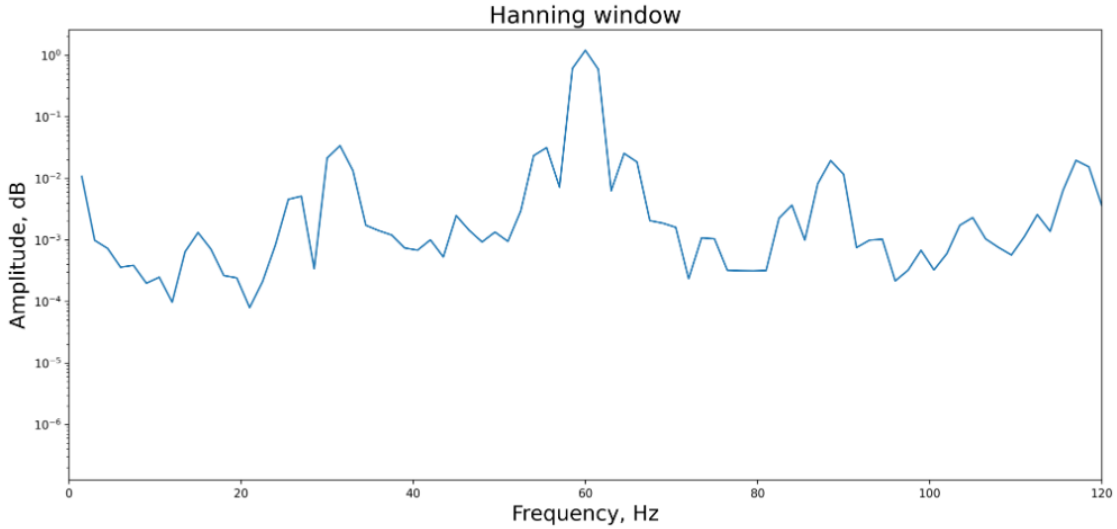


Figure 14: Hanning window current frequency spectrum at 3 BRB

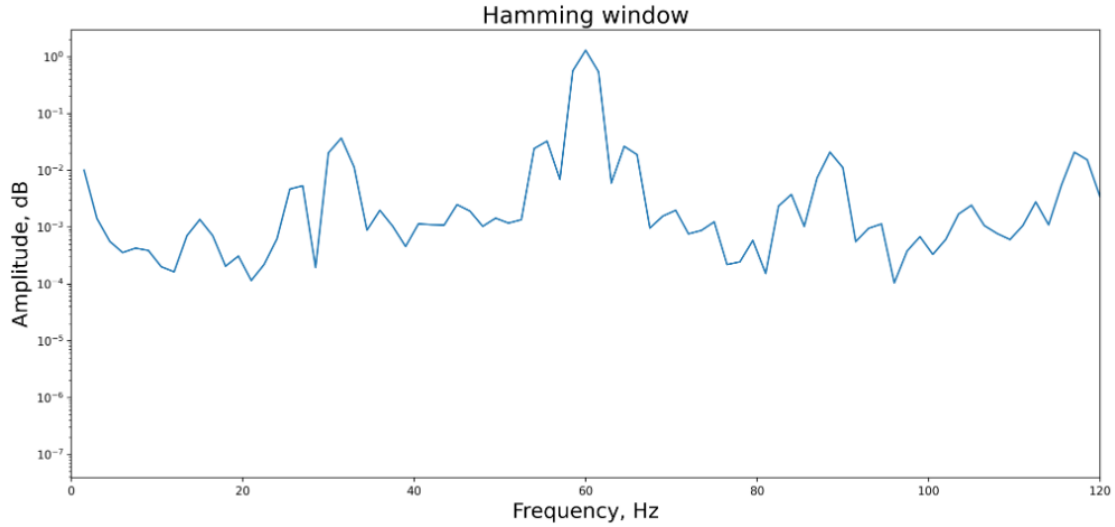


Figure 15: Hamming Window current frequency spectrum at 3 BRB

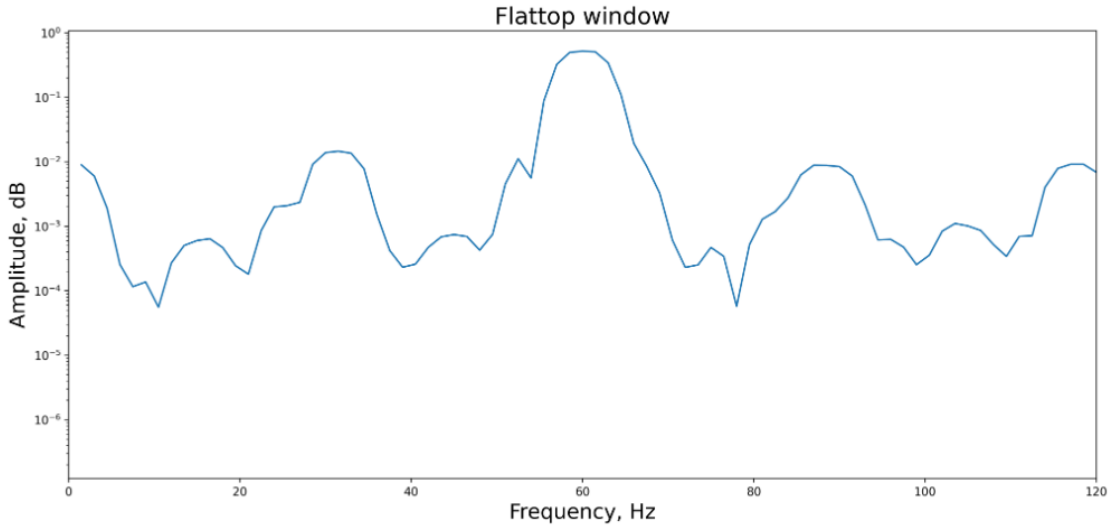


Figure 16: Flattop Window current frequency spectrum at 3 BRB

Application of FFT windowing functions is completed using a window length of 40 electrical cycles. After a proper study of the frequency spectrum formed by the different FFT windowing functions between the healthy state motor and the motor under 3 BRBs at full load, few observations have been made. The observations are:

- Alterations of the amplitudes of certain frequency components are seen.
- Additional frequency peaks had appeared in the spectrum corresponding to sidebands or harmonics generated by the Broken Rotors Bar faults.
- Increased harmonic content, especially around the sidebands and the harmonic components.

4.2 Window Length

The window length, also known as the number of samples in the time-domain signal that are included in the window may have an impact on the performance of windowing functions in FFT analysis.

To see how the window length affects the performance of the windowing functions, a similar FFT analysis is executed by extending the window length up to 200.

In examining the frequency spectrum under optimal conditions and with a motor experiencing three broken rotor bars at full load (100%), a comparison was conducted using various windowing functions in FFT analysis.

Figure 17, 18, 19, 20, and 21 provides the frequency spectrum of the healthy state motor at full load and Figure 22, 23, 24, 25, and 26 provides the frequency spectrum of the motor at 3BRBs.

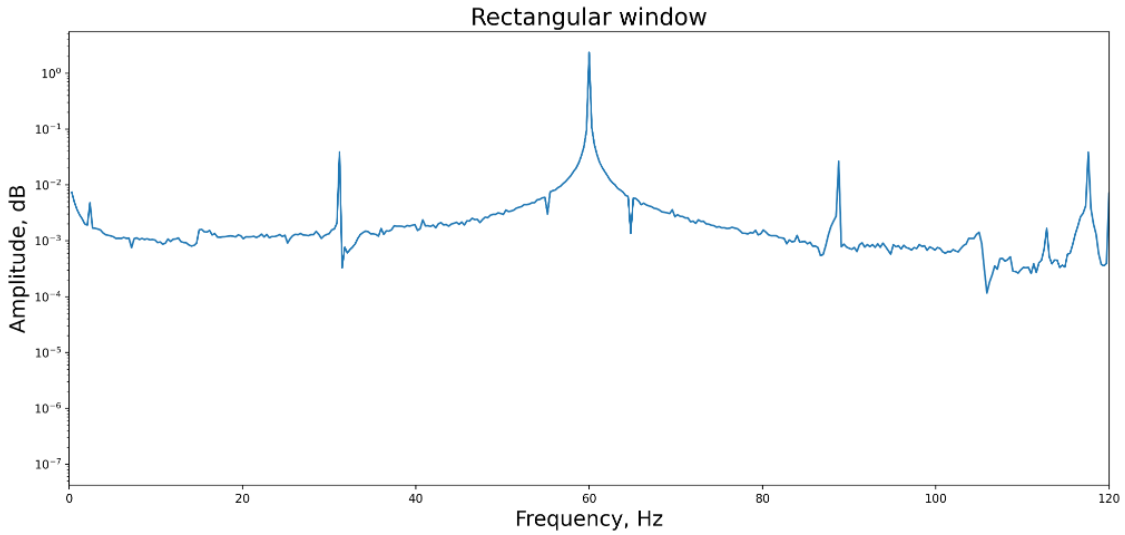


Figure 17: Rectangular window at healthy state motor under full load

4.3 Frequency Spectrum at Healthy State

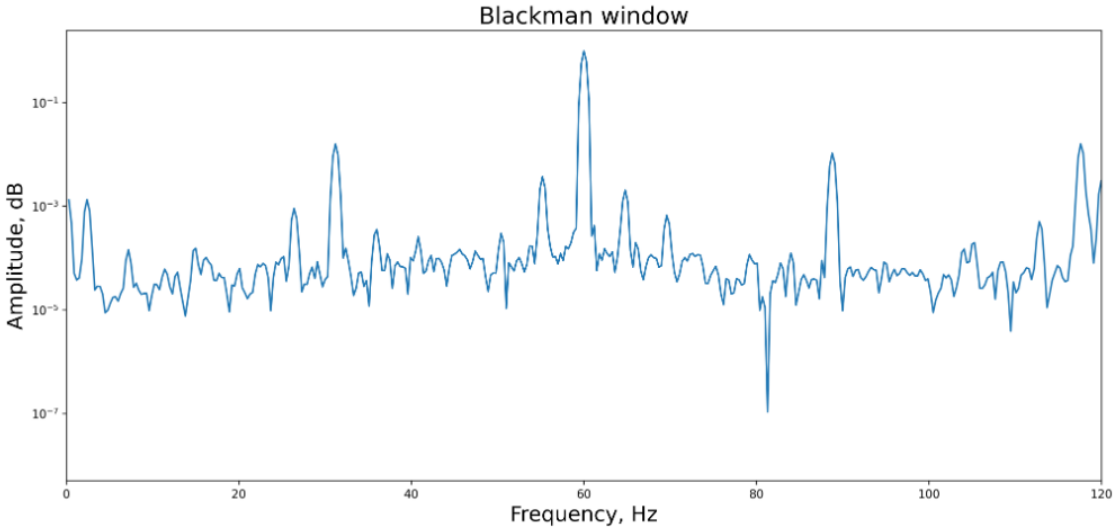


Figure 18: Blackman window at healthy state motor under full load

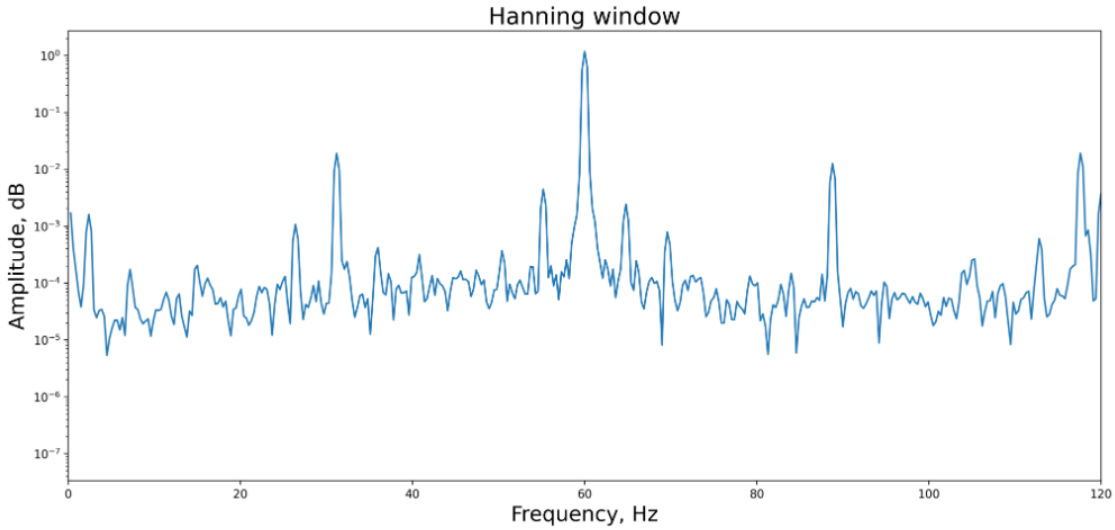


Figure 19: Hanning window at healthy state under full load

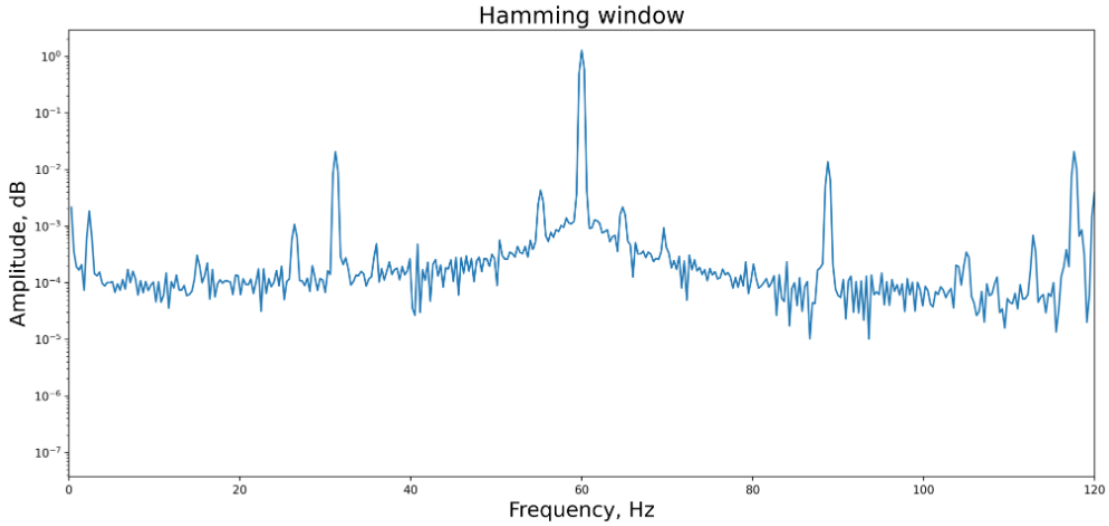


Figure 20: Hamming window at healthy state under full load

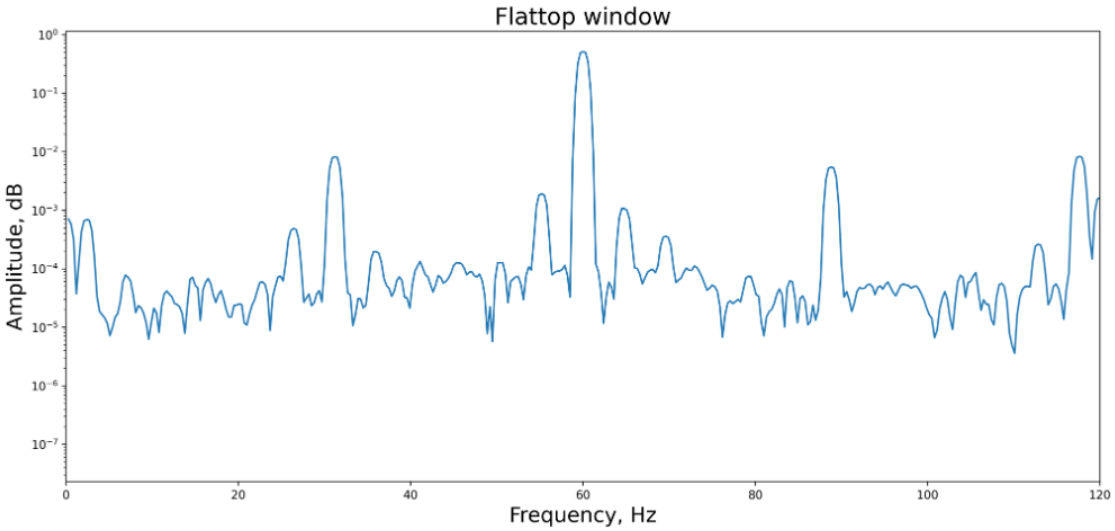


Figure 21: Flattop window at healthy state under full load

4.4 Frequency Spectrum at 3BRBs

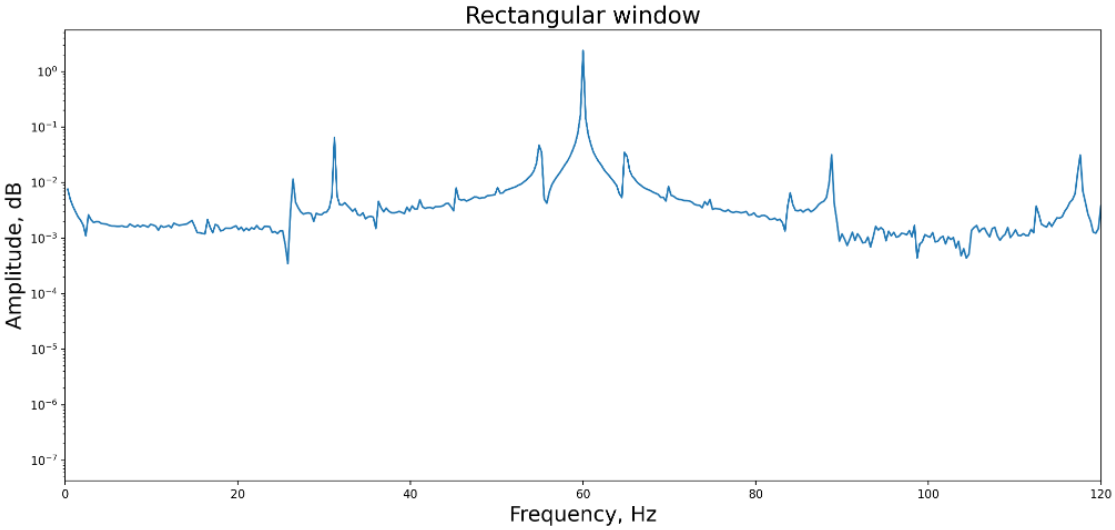


Figure 22: Rectangular window at 3 BRBs under full load

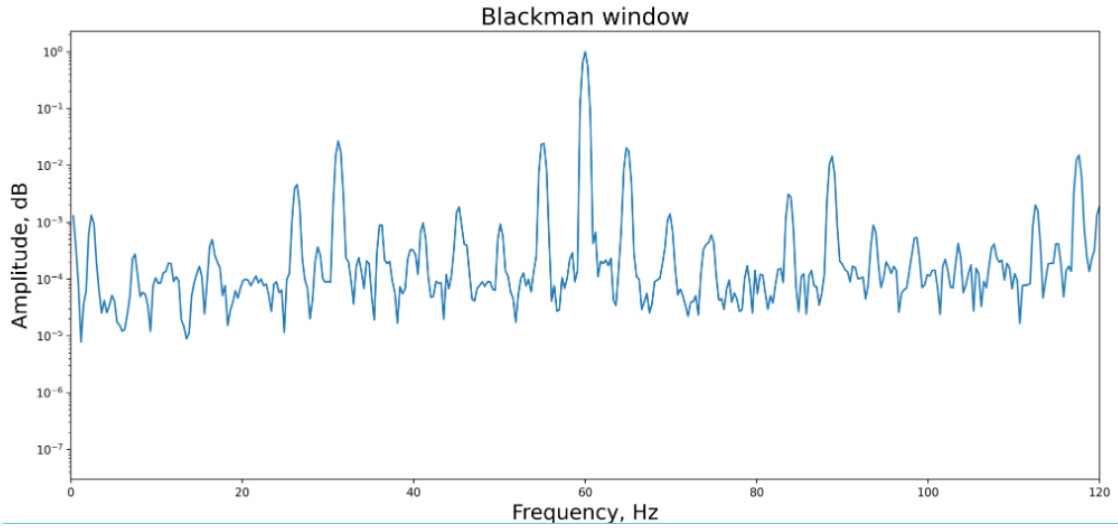


Figure 23: Blackman window at 3 BRBs under full load

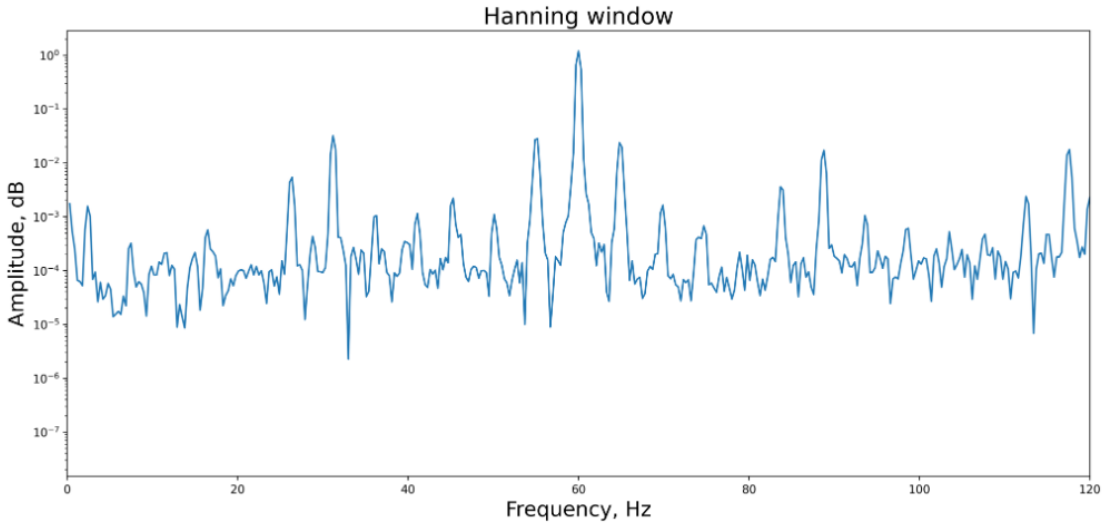


Figure 24: Hanning window at 3 BRBs under full load

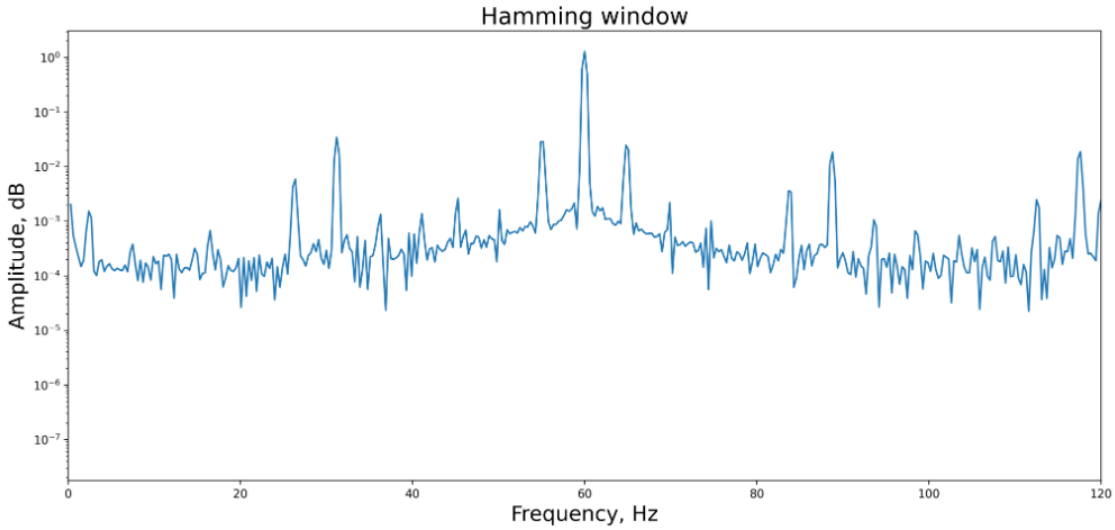


Figure 25: Hamming window at 3 BRBs under full load

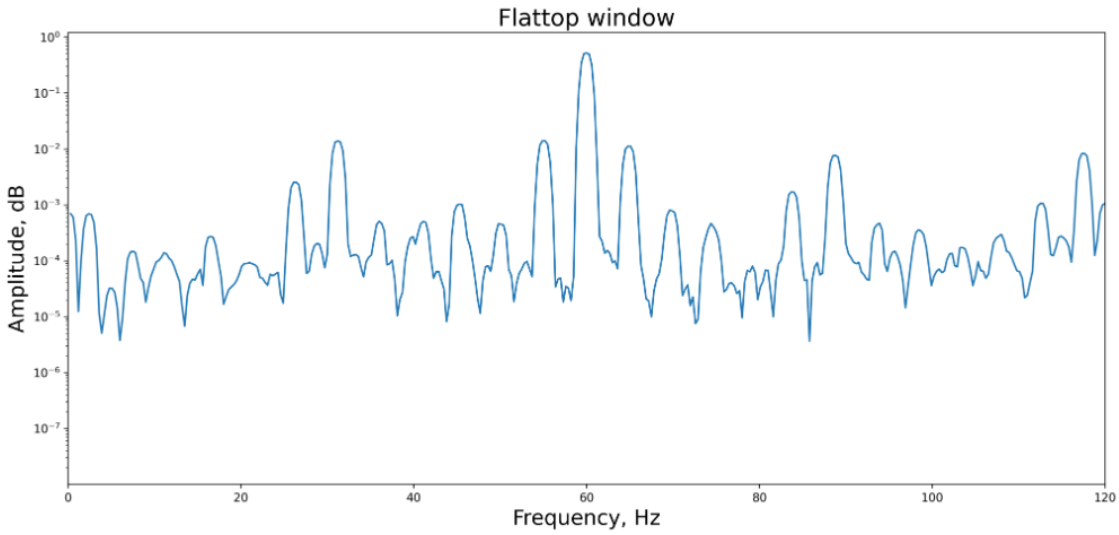


Figure 26: Flattop window at healthy state under full load

After conducting a comprehensive study on the frequency spectra generated by various FFT windowing functions applied with extended window lengths of up to 200 electrical cycles, proper observations were made regarding the comparison between a healthy motor shown the Figure 7 and the one operating at three broken rotor bars under full load.

During the analysis of the frequency spectra using different FFT windowing functions, it was noted that the amplitudes of the sidebands and the number of harmonic frequency components exhibited an increase when the motor operated under the condition of 3BRBs. This process indicates a pronounced deviation from the healthy state. Additionally, in healthy state motors, the sideband peaking frequencies were observed to be significantly lower than those observed in the motors with 3BRBs which suggests the clear alternation in the frequency characteristic due to Broken Rotor Bars. Figure 27 shows the comparison of frequency spectrum formed by Hanning window at healthy state and 3BRBs under full load.

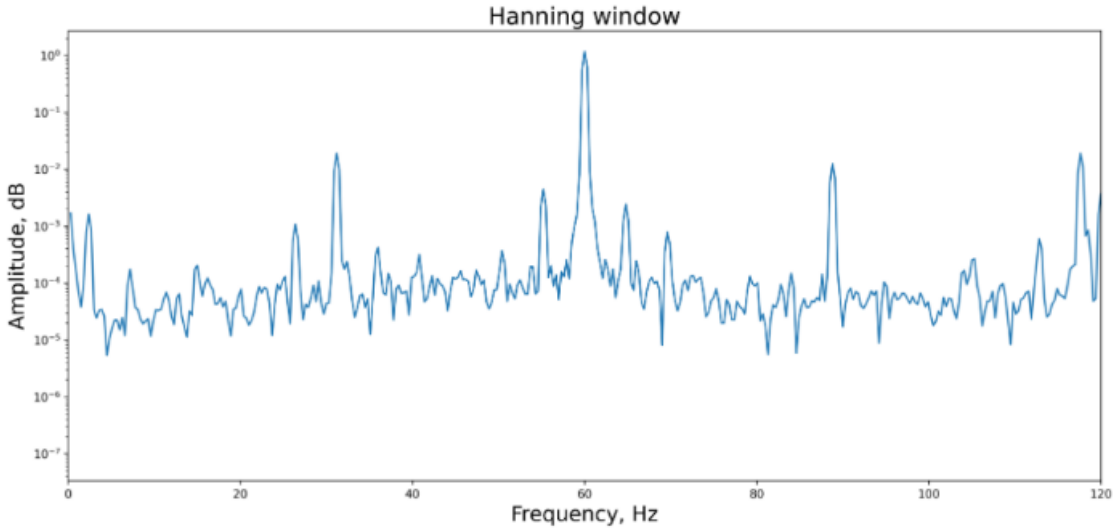


Figure 27: Rectangular window at 3 BRBs under full load

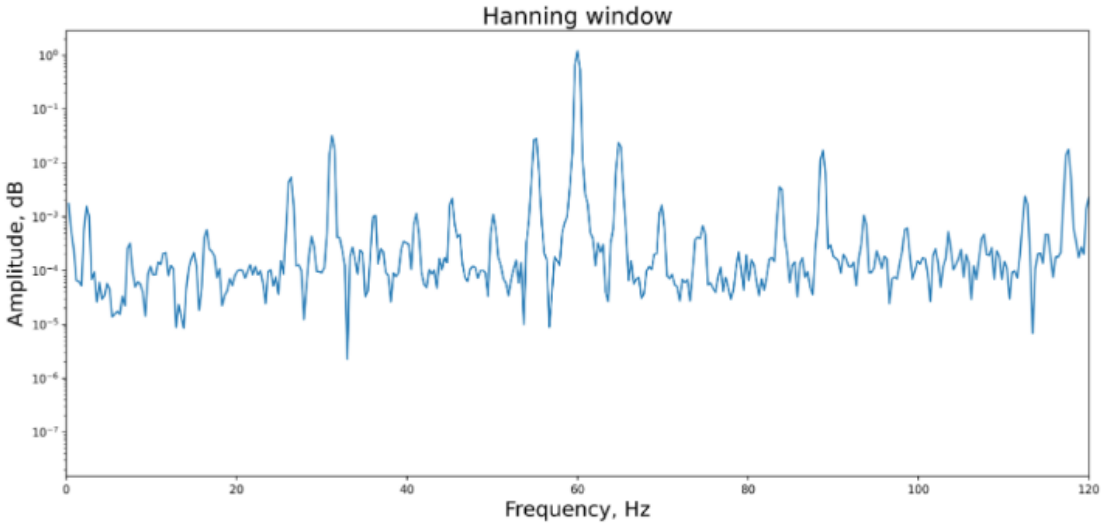


Figure 28: Comparison of (a) healthy state and (b) 3BRBs frequency spectrum at full load

Furthermore, it was observed that longer window length generally results in better frequency resolution compared to shorter ones. This is attributed to their ability to mitigate spectral leakage by smoothly tapering the signal at the edges resulting in narrower main lobes. Figure 28 shows the comparison of frequency spectrum formed by Hanning window using two different widow lengths when motor suffers under 3 BRBs at full load.

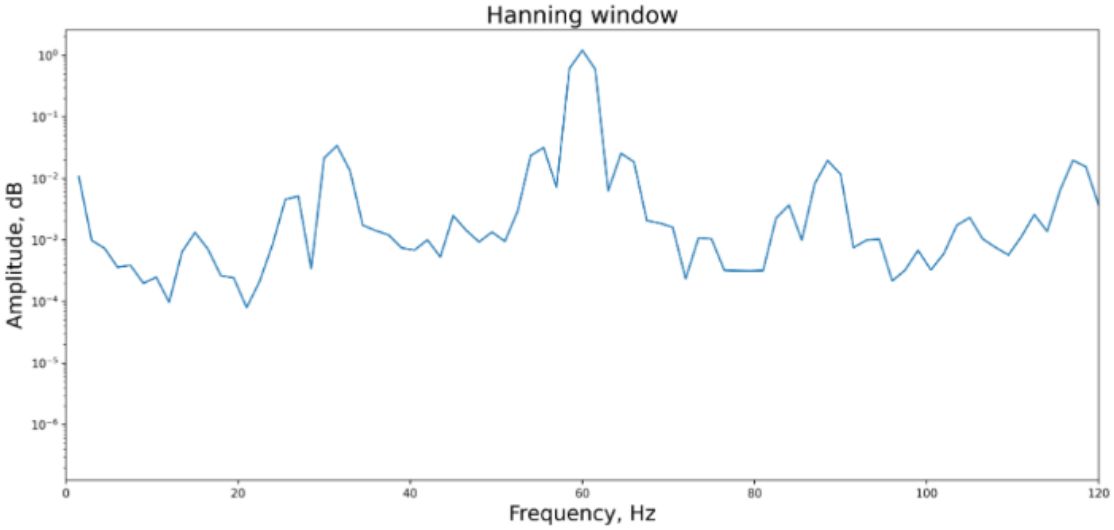


Figure 29: Comparison of two window-length spectrums at 25%

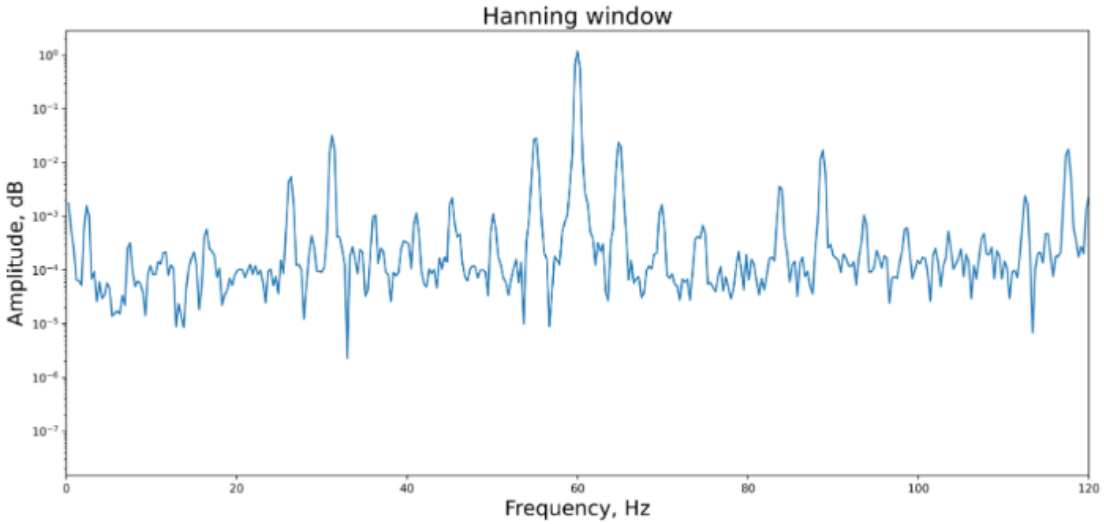


Figure 30: Comparison of two window-length spectrums at 100%

4.5 Two-test comparison

After studying the research written by Culbert and Rhodes, one of the major problems with identifying the rotor cage winding breaks is that other mechanical devices in the rotor system can also produce symmetrical current components around the fundamental 50/60 Hz supply current. To confirm that the symmetrical current sidebands are from cage winding breaks, a "two-test comparison" is used. This involves conducting two current signature analysis (CSA) tests at different loads (at least 40% difference if possible but the lower load must be well above no-load). If the symmetrical components are from mechanical sources, there would be much frequency change with load. However, if they are from broken cage windings, their frequencies will change significantly with load due to slip variations [13].

The "two-test comparison" is particularly useful for differentiating between symmetrical fundamental current sidebands due to cage winding breaks and those due to speed-reducing mechanical devices [13]. A comparison of the current spectra for the two tests between high load (100%) and low load (25%) under 3 BRB is shown in Figure 10. From this, it can be easily seen that the

side-band peaking frequencies under 25% load level are located much closer to the fundamental frequency while the side-band peaking frequencies under 100% load level are far from the fundamental frequency. This could be due to the presence of broken rotor bars which causes additional frequency components in the current spectrum. The abbreviations indicated in the figure are as follows: f represents the fundamental frequency, lsb denotes the left sideband and rsb stands for the right sideband.

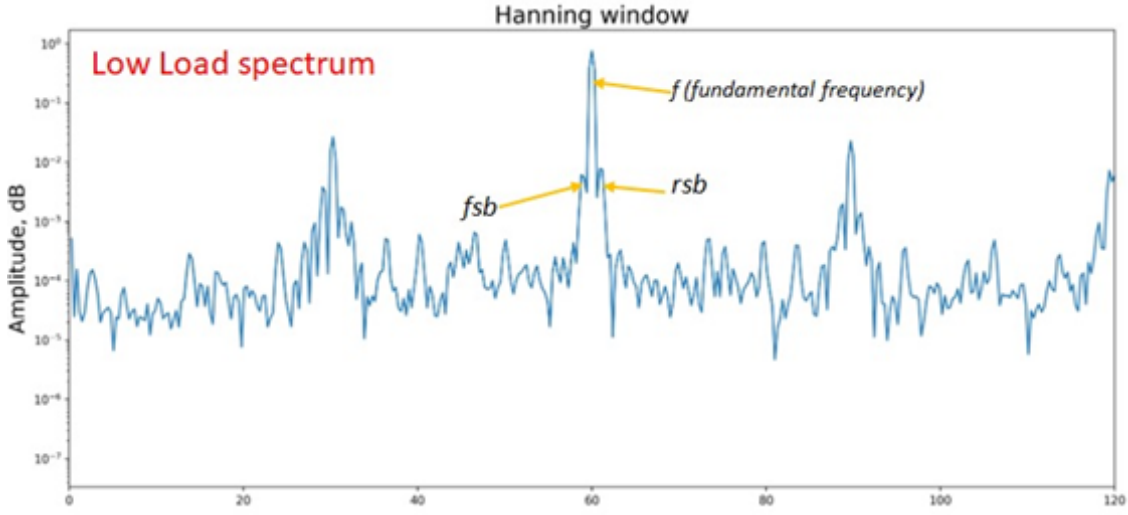


Figure 31: Current signature components in two-test comparison of a motor with 3BRB under 25% Load level

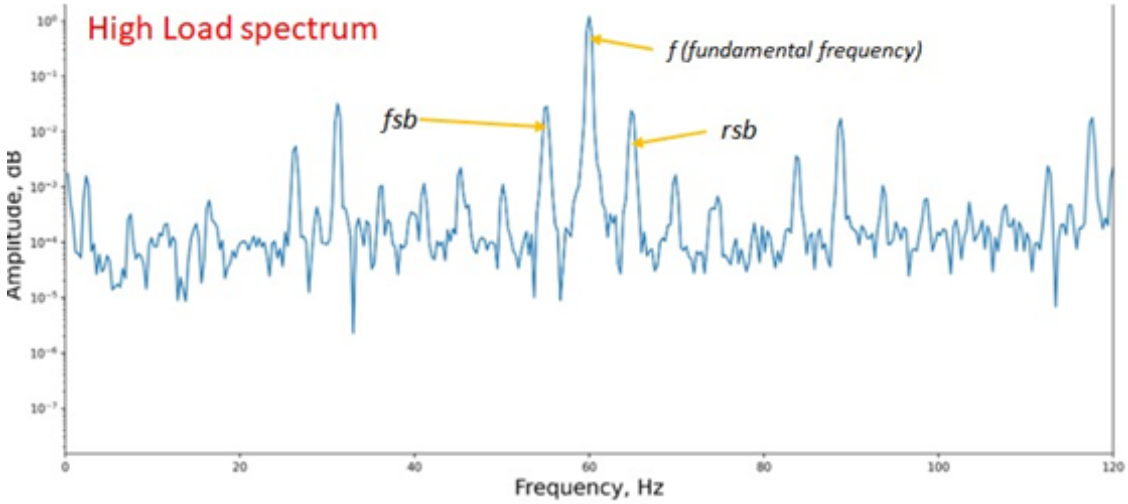


Figure 32: Current signature components in two-test comparison of a motor with 3BRB under 100% Load level

5 Result and Discussion

5.1 Result

The preliminary analysis of the article proposes significant variations in the fault detection performance using different FFT windowing functions. Each windowing function exhibits unique char-

acteristics in terms of spectral leakage, frequency resolution, and side-lobes levels which influence their suitability for fault detection applications.

Findings from the article indicate that the Hanning and Blackman windowing functions tend to provide better, and clearer frequency resolutions compared to the other windowing functions.

Operating conditions of the induction motor and severities of broken rotor bar faults (BRBs) may impact the features of the current frequency spectra, making it either more or less challenging to identify and differentiate the broken rotor bar faults in the spectrum.

As the load increases the frequency spectrum may change, affecting the visibility of the fault-related features. Similarly, if the severity of the Broken Rotor Bar (BRB) fault increases then the amplitude and the frequency of the sidebands may differ.

As the load increases, the effects of the broken rotor bars become more pronounced, leading to greater separations between the sideband frequencies.

5.2 Discussion

The results of the study have important applications for the development of fault detection algorithms and for the motor maintenance practices where most of the induction motors are being used. Properly comparing the performance of the different windowing functions in detecting broken rotor bar faults, this report contributes to a better understanding of how the current frequency spectrum changes during the occurrence of the BRB faults and it enables a clear idea of the factors influencing the fault detection performance in induction motors.

The findings suggest that the choice of windowing function can significantly impact the effectiveness of fault detection while analyzing the accuracy and reliability of the motor in the frequency spectra. Furthermore, variations in load level and fault severity highlight how important it is to have smart systems that can recognize faults and adjust to the changes in how things are working.

Overall, this study provides valuable insights into the comparative analysis of Broken Rotor Bar (BRB) fault detection using different FFT windowing functions and underscores the need for further research to develop robust motors.

6 Conclusion

In conclusion, the widespread use of induction motors in industrial applications underscores the importance of effectively detecting and diagnosing faults to maintain performance and prevent downtime of the motor. Broken Rotor Bar faults pose a significant threat to the squirrel cage induction motor, leading to rotor imbalance, increased vibration, and reduced efficiency.

This paper conducted a comparative analysis of BRB fault detection in induction motors focusing on the effectiveness of different windowing functions. Through the utilization of Hanning, Hamming, Blackman, and Flattop windowing functions alongside Fast Fourier Transform (FFT) techniques.

The study shows that different windowing functions have varying effectiveness in detecting faults in induction motors, like BRBs. Understanding which windowing functions work best can help develop better fault detection strategies, making motors more reliable and efficient for industrial applications.

Acknowledgement

The team would like to thank Professor Anouar Belahcen and Semen Koveshnikov, Doctoral Researcher from the Department of Electrical Engineering and Automation of Aalto University, Finland for guiding the team.

References

[1] O. E. Hassen, M. Amer, A. K. Abdelsalam, and B. W. Willaims, "Induction Motor Broken Rotor Bar Fault Detection Techniques Based on Fault Signature Analysis," *IET Electric Power Applications*, vol. 12, no. 7, p. 895, 2018.

[2] C. Marcelo, J. P. Fossatti, and J. I. Terra, "Fault Diagnosis of Induction Motors Based on FFT," in *Fourier Transform - Signal Processing*, S. Salih, Ed., InTech, 2012. [Online]. Available: `https://www.intechopen.com/books/fourier-transform-signal-processing/fault-diagnosis-of-induction-motors-based-on-fft`

[3] S. Randy, N. Ertugoul, W. L. Soong, D. A. Gray, C. Hansen, and J. Grieger, "Broken Rotor Bar Fault Detection in Induction Motors Using Starting Current Analysis."

[4] I. Culbert and W. Rhodes, "Using Current Signature Analysis Technology to Reliably Detect Cage Induction Motors," *IEEE*, 2005.

[5] R. J. R. Troncoso Sr., "Multirate Signal Processing to Improve FFT-Based Analysis for Detecting Faults in Induction Motors," *IEEE Transactions on Industrial Informatics*, vol. 13, no. 3, p. 1291, 2017.

[6] S. Koveshnikov, "Machine Learning Methods for Induction Motor Fault Detection," Master's thesis, pp. 16–18, 2023.